

MOVING LOAD ANALYSIS OF SUBMERGED FLOATING TUNNELS

M. Shahmardani, J. Mirzapour, Ch. Gheytratmand, S. Tariverdilo*

Department of Civil Engineering, University of Urmia, Urmia, Iran
Shahmardani.mahdieh@gmail.com, J.mirzapour@iausaghez.ac.ir, Ch.gheytratmand@urmia.ac.ir,
S.tariverdilo@urmia.ac.ir

*Corresponding Author

(Received: November 24, 2010 – Accepted in Revised Form: January 19, 2012)

doi: 10.5829/idosi.ije.2012.25.01c.03

Abstract The concept of floating submerged tunnels becomes increasingly attractive idea to cross the straits. The structural solution in these bridges includes buoyancy force on tunnel body plus tension in mooring tethers. This paper investigates the effect of submergence on the dynamic response of submerged floating tunnels due to moving load. The inertial effect of the fluid on the submerged structure is accounted for by evaluating the added mass in deep and shallow waters. Then the effect of moving load velocity on the dynamic amplification factor for mid span displacement is evaluated. The results show that while the inertial effect of fluid reduces the critical velocity, closely spaced tethers provides a means to increase this velocity and could be used to control the moving load effect. Although increasing the tether stiffness increases the critical velocity, at the same time it results in the escalation of the impact factor.

Keywords Fluid-structure interaction; Floating submerged tunnel; Moving load; Added mass; Shallow water.

چکیده جابه‌جایی طبیعی ایده استفاده از پل‌های غوطه‌ور برای عبور از تنگه‌های عمیق به تدریج به ایده جذابی تبدیل می‌شود. عملکرد سازه‌ای این پل‌ها مبتنی بر استفاده از نیروی شناوری آب به علاوه کشش در مهارهای کششی می‌باشد. این مقاله به بررسی اثر غوطه‌وری در آب روی پاسخ دینامیکی تونل تحت بار متحرک می‌پردازد. اثرات اینرسی آب در پاسخ تونل با محاسبه جرم افزوده سیال در حالت آب‌های عمیق و کم عمق بررسی شده است. پس از تعیین جرم افزوده، اثر بار متحرک روی تغییر مکان وسط دهانه ارزیابی شده است. نتایج نشان‌گر آن است که در حالی که اینرسی ناشی از جرم افزوده سیال منجر به کاهش سرعت بحرانی می‌گردد، کاهش فاصله مهارهای کششی منجر به افزایش سختی تونل شده و سرعت بحرانی را افزایش می‌دهد. اگرچه افزایش سختی مهارهای کششی سرعت بحرانی را افزایش می‌دهد، ولی در عین حال منجر به افزایش ضریب ضربه می‌گردد.

1. INTRODUCTION

Overcoming the technological problems, the concept of submerged floating tunnel (SFT) in comparison with long span cable stayed and suspension bridges, becomes an increasingly viable alternative to cross the sea straits. With the experience obtained in the design and construction of tension leg platforms in offshore structures, now it is possible to overcome the technological problems in adoption of SFTs as an alternative solution for crossing the straits. Minimizing the environmental and pollution impact [1], SFTs now is considered as main alternative for some

waterway crossing projects including: Høgsfjorden crossing in Norway, the Messina strait in Italy and the northern exchange axis in Japan [2]. In this concept the tunnel moored to the sea bed via tethers is maintained in its position by a combination of tension force in tethers and buoyancy force on the tunnel body. Hydrodynamic forces could be developed on the tunnel due to different sources such as surface waves, ground shaking or traffic moving load.

Remesth et al. [3] considering the fluid-structure interaction (FSI) developed a finite element solution for the response of submerged floating tunnels due to wind driven surface waves.

They found that wave direction has a dominant effect on the response amplitude. Di Pilato et al. [4] accounting for multi support excitation developed a numerical solution for the response of the submerged floating tunnel. They mainly focused on finite element modeling of nonlinear behavior of anchoring tethers. Fleischer and Park [5] investigated the response of a beam floating on the water surface due to moving load. Deriving the change in the frequency of first mode as a function of the water depth, they studied the response of the floating beam under moving vehicle. Paik et al. [6] using boundary element method in a two dimensional model developed the added mass and damping coefficient for a submerged floating tunnel. Then, they used this added mass and damping to investigate the response of the submerged bridge in three dimensional model under wave loading.

Assuming the fluid as incompressible and inviscid, it is possible to treat the flow field using a scalar potential function. This facilitates the evaluation of added mass, which simulates the inertial effect of the fluid as it is accelerated by the structure, and greatly simplifies the treatment of FSI problem. Yadykin et al. [7] reviewing various methods to calculate the added mass for plates submerged in the fluid, studied the effect of plate aspect ratio on the added mass of different modes. Accounting for the proximity of sea bed or free surface in zero frequency excitation Clarke [8, 9] used conformal mapping to derive the added mass for circular or elliptic sections. Employing finite difference method Zhou et al. [10] derived the added mass considering the effect of shallow and narrow waters. They derived the added mass for different modes of vibration.

Dynamics of structures excited by moving load is subject of interest for well over a century. The literature in this regard could be classified by the way they treat the dynamics of system subjected to moving load, moving mass or moving sprung mass models [11]. However, as it was shown by Pesterev et al. [12], there is no meaningful difference between results of these models for smooth road surface bridges.

In this study, decomposing the response of the tunnel in terms of its eigenfunctions, the effect of FSI on the response is accounted for using the concept of added mass. Deriving analytically the added mass for the case of deep water, the effect of

proximity to free surface or sea bed is evaluated by a finite element solution for the potential function in shallow water. Then, the effect of moving load and tether spacing and stiffness on the response is evaluated.

2. FORMULATION

Figure 1 depicts the typical shape of a submerged tunnel as anchored to the sea floor by means of tethers. To simplify the moving load treatment, in this study moving load is treated as moving force. The dynamic equilibrium equation for simultaneous application of fluid pressure and moving load, and considering only the vertical oscillation of the submerged tunnel will be:

$$m \frac{\partial^2 w}{\partial t^2} + EI \frac{\partial^4 w}{\partial x^4} + kw = P\delta(x - vt) + F \quad (1)$$

where w denotes the tunnel deflection from static equilibrium position, m and EI are mass density and flexural stiffness of the tunnel, respectively; and k is the equivalent linear stiffness of the mooring tethers. In this equation P is magnitude of moving load, and F is the external force on the tunnel due to fluid pressure. In this equation ignoring the mass of moving particle, it is treated as a moving load.

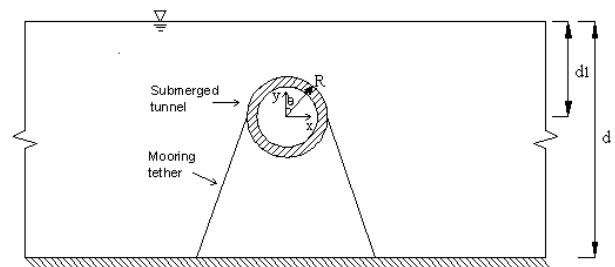


Figure 1. Schematic view of submerged floating tunnel.

For slender bodies in which their length in one direction is considerably longer than the other two dimensions, it is common to derive three dimensional added mass by integrating the two dimensional added mass along the member length. In other words, it is assumed that the inertial contribution of the fluid remains constant along body length. This makes it possible to consider only two dimensional fluid field.

As the motion of water particles compared to the SFT diameter is small, it is anticipated that water velocity be small, and accordingly drag force be negligible in comparison with inertial force [2]. Therefore, potential theory can be used to evaluate the fluid loading on the SFT. An incompressible and inviscid fluid is irrotational, and the fluid field can be treated by scalar potential function ϕ satisfying the Laplace equation:

$$\nabla^2 \phi = \frac{\partial^2 \phi}{\partial r^2} + \frac{1}{r} \frac{\partial \phi}{\partial r} + \frac{1}{r^2} \frac{\partial^2 \phi}{\partial \theta^2} = 0 \quad (2)$$

where r and θ are polar coordinates. For infinite fluid domain the potential function should satisfy radiation boundary condition together with boundary condition associated with compatibility of velocity between fluid and structure:

$$\lim_{r \rightarrow \infty} \phi = 0, \quad \lim_{r \rightarrow \infty} \frac{\partial \phi}{\partial r} = 0, \quad \left(\frac{\partial \phi}{\partial r} \right)_{r=R} = \frac{\partial w}{\partial t} \cos \theta \quad (3)$$

where R is outer radius of the tunnel. The admissible solution for the potential function satisfying the boundary conditions of Equation (3) will be:

$$\phi(r, \theta) = -\frac{\partial w}{\partial t} \frac{R^2}{r} \cos \theta \quad (4)$$

Assuming small velocities, and employing Bernoulli's equation for unsteady fluid flow, the hydrodynamic force could be calculated by integrating the fluid pressure on tunnel's wet surface as :

$$F = -\rho_f \pi R^2 \frac{\partial^2 w}{\partial t^2} \quad (5)$$

In other words, the added mass for circular tunnel becomes

$$m_a = \rho_f \pi R^2 \quad (6)$$

Therefore, the equilibrium equation for tunnel reduces to:

$$(m + m_a) \frac{\partial^2 w}{\partial t^2} + EI \frac{\partial^4 w}{\partial x^4} + kw = P \delta(x - vt) \quad (7)$$

Using eigenfunction expansion in terms of beams orthogonal mode shapes ($\psi_n(x)$), we could

decompose the tunnel deflection and forcing function:

$$w(x, t) = \sum_n \psi_n(x) T_n(t) \quad (8)$$

$$P \delta(x - vt) = \sum_n \psi_n(x) P_n(t)$$

Deploying this in Equation (1) yields:

$$(m + m_a) \sum_n \psi_n(x) \ddot{T}_n(t) + \sum_n [EI \psi_n^{iv}(x) + k \psi_n(x)] T_n(t) = \sum_n \psi_n(x) P_n(t) \quad (9)$$

Multiplying both sides of Equation (9) by $\psi_i(x)$ and integrating along tunnel length, it reduces to:

$$m_i \ddot{T}_i(t) + k_i T_i(t) = f_i(t) \quad (10)$$

where

$$m_i = (m + m_a) \int_0^l \psi_i^2(x) dx \quad (11)$$

$$k_i = \int_0^l [EI \psi_i^{iv}(x) + k \psi_i(x)] \psi_i(x) dx$$

$$f_i = P \psi_i(vt)$$

Considering the case of hinged boundary condition which is common boundary condition for SFTs (see next section), the analytical solution for tunnel mid span displacement becomes:

$$w \left(x = \frac{l}{2} \right) \quad (12)$$

$$= w_{st} \sum_{n=1}^{\infty} \frac{1}{n^4 \left(1 - \frac{\omega_{bn}^2}{\omega_n^2} \right)} \left(\sin(\omega_{bn} t) - \left(\frac{\omega_{bn}}{\omega_n} \right) \sin(\omega t) \right)$$

where

$$\omega_n = \sqrt{\frac{EI(n\pi/l)^4}{m + m_a}}, \quad \omega_{bn} = \frac{n\pi v}{l} \quad (13)$$

Here ω_n and ω_{bn} denote the n th natural and driving frequencies and w_{st} is the static deflection due to load application at mid-span.

2.1. Shallow Water Effect Proximity of the tunnel to the seabed or free surface affects the inertial contribution of the fluid. To develop a numerical solution for Laplace equation a finite element discretization as depicted in Figure 2 is

used. The Laplace equation in Cartesian coordinate reads as:

$$\frac{\partial^2 \varphi}{\partial x^2} + \frac{\partial^2 \varphi}{\partial y^2} = 0 \quad (14)$$

Using $\eta(x,y)$ as weight function and adopting the weighted residual approach leads to:

$$\int_{\Omega} \eta \left(\frac{\partial^2 \varphi}{\partial x^2} + \frac{\partial^2 \varphi}{\partial y^2} \right) dx dy = 0 \quad (15)$$

Using Green theorem, the weak form becomes:

$$\int_{\Omega} \left(\frac{\partial \eta}{\partial x} \frac{\partial \varphi}{\partial x} + \frac{\partial \eta}{\partial y} \frac{\partial \varphi}{\partial y} \right) d\Omega - \int_{\Gamma} \eta \frac{\partial \varphi}{\partial n} d\Gamma = 0 \quad (16)$$

Now, decomposing φ in terms of interpolation functions φ_i , we have:

$$\varphi(x, y) = \sum_i a_i \varphi_i(x, y) \quad (17)$$

By tuning φ_i such that they have zero value at nodes other than i and be equal to one for node i , parameters a_i will be value of potential function at node i . Adopting the same interpolation functions also as weight functions (Galerkin method) leads to:

$$\sum_i a_j \int_{\Omega} \left(\frac{\partial \varphi_i}{\partial x} \frac{\partial \varphi_j}{\partial x} + \frac{\partial \varphi_i}{\partial y} \frac{\partial \varphi_j}{\partial y} \right) d\Omega = \int_{\Gamma} \sum_i \varphi_i \frac{\partial \varphi}{\partial n} d\Gamma \quad (18)$$

$i, j = 1, \dots, N$

which could be rewritten as:

$$\sum_i k_{ij} a_j = f_i \quad i, j = 1, \dots, N \quad (19)$$

where we have:

$$k_{ij} = \int_{\Omega} \left(\frac{\partial \varphi_i}{\partial x} \frac{\partial \varphi_j}{\partial x} + \frac{\partial \varphi_i}{\partial y} \frac{\partial \varphi_j}{\partial y} \right) d\Omega \quad (20)$$

$$f_i = \int_{\Gamma} \varphi_i \frac{\partial \varphi}{\partial n} d\Gamma$$

After imposing boundary conditions, evaluating integrals and assembling the load and stiffness matrixes, this reduces to a set of algebraic equations, that its solution gives the value of potential function value at each node. As depicted in Figure 2, the finite element discretization

employs triangular elements. The boundary conditions for this boundary value problem are:

$$\begin{aligned} \frac{\partial \phi}{\partial x} \Big|_{x=\pm l} &= 0, & \frac{\phi}{r} \Big|_{r=R} &= \frac{\partial w}{\partial t} \cos \theta_i \\ \phi \Big|_{y=d_1} &= 0, & \frac{\partial \phi}{\partial y} \Big|_{y=-d_2} &= 0 \end{aligned} \quad (21)$$

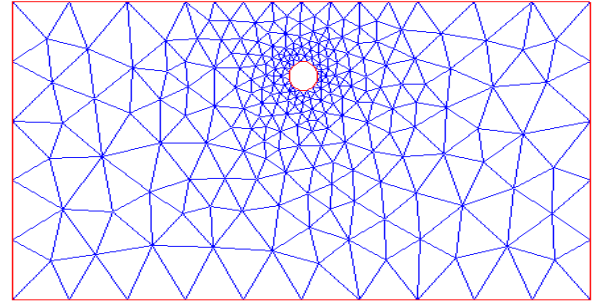


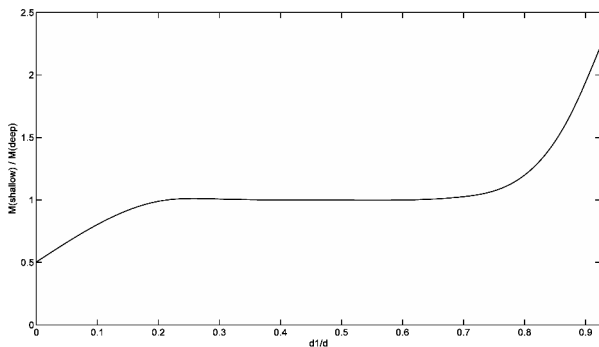
Figure 2. Typical finite element discretization of fluid field in the case shallow water.

where boundary condition at free surface ($y=d_1$) follows those of Zhou et al. for heave motion.

Figure 3 shows the variation of the ratio of added mass in shallow water to deep water as a function of submergence depth (d_1). The added mass for the case of deep water could be evaluated using Equation (6). Examination of this figure reveals that for the tunnel near the sea bed, the inertial effect of surrounding water increases rapidly, while for d_1/d between 0.2 and 0.7 it remains essentially constant, close to its value for deep water. On the other hand, for the tunnel near water surface, the added mass reduces. To accommodate the passage of ships, it is common in the design of SFT's to use a submergence depth of about 30 m. Therefore, accounting for shallow water effect the added mass usually will be greater or at least equal to that in deep waters. In Table 1, the value of added mass for zero submergence depth is compared with numerical results of Zhou et al. and analytical results of Newman [13]. On the other hand, for tunnel near the sea bed the ratio of added mass in shallow water to that in deep water is calculated as 2.25; this is comparable with analytically derived value of 2.29 by Garrison [14] which is also suggested by DNV [15].

TABLE 1. Comparison of added mass value for $d_1/d=0$

| | Ratio of added mass of $d_1/d=0$ to added mass of deep water |
|------------------|--|
| Present study | 0.50 |
| Zhou et al. [10] | 0.50 |
| Newman [13] | 0.50 |

**Figure 3.** Evolution of added mass with submergence depth for shallow water.

3. SIMULATION RESULTS

SFTs have two elements, a submerged floating tunnel and a land bored tunnel. To accommodate the possible differential settlement between these elements a specially detailed joint is required between submerged and bored elements allowing for relative rotation and axial movement between adjacent parts. Therefore, the boundary condition for SFT in all of the following simulations is assumed to be hinged one.

Overall dimensions of SFTs are determined by required allowance for equipments and traffic lanes. At the same time, to avoid the need to the supporting columns, the overall dimension should satisfy the requirement that the buoyancy force should exceed the sum of dead weight and traffic loads. This results in residual buoyancy. In the design of SFTs, the residual buoyancy controls the force in anchors and tunnel body. Reduction in this residual buoyancy can be obtained by using ballast to increase the dead weight of the tunnel. By this way it is possible to increase the anchors spacing. Remseth et al. [3] used an anchors spacing of about 300 m for their study on HØgsfjorden crossing. On the other hand, Di Pilato et al. [4] used

closely spaced anchors comparable to a continuous elastic stiffness in their study on the Messina waterway.

Currently there are three main candidates for adoption of submerged floating tunnel as viable solution for crossing the sea straits. In the case of HØgsfjorden crossing which is 1400 m long with maximum water depth of 150 m, the inner diameter of the tunnel is 9.5 m and the tunnel will be placed at about 25 m below the water surface. The Messina crossing is about 3000 m long and the maximum water depth is 350 m. The northern exchange axis in Japan includes three SFT segments with length between 7 to 27 Km.

Considering the above mentioned real world applications, the tunnel cross sectional dimension is selected such that it models a concrete tunnel with internal diameter of 15 m and thickness of 1 m (Table 2). To study the effect of tunnel length on the response, its length is varied from 1000 to 3000 m, with an increment of 500 m. Also the effect of closely and largely spaced anchors on the response of the SFT is investigated. To evaluate the dynamic response of the SFT under moving load the analytical solution of Equation (12) and to assess the change in the added mass of the water due to proximity to the sea bed or the free surface discretized Equation (19) together with boundary conditions of Equation (21) are employed. The main parameters controlling the response are SFT length, proximity to the sea bed or the free surface, and tether stiffness. In the following the effect of these parameters on the response are investigated.

TABLE 2. Parameters used in the analyses

| Parameter | Value |
|---------------------------|-----------------------|
| EI (KN.m ²) | 3.35×10^{10} |
| k (KN/m/m) | 50 |
| R (m) | 7.5 |
| d (m) | 100 |

Figures 4 shows the variation of impact factor versus velocity for tunnels with and without accounting for FSI in deep water and assuming no stiffness for anchoring tethers ($k=0$). Ignoring tethers stiffness, the critical speed (corresponding to maximum impact factor) is very low. Taking into account the added mass effect of surrounding water (deep water) further reduces the critical velocity.

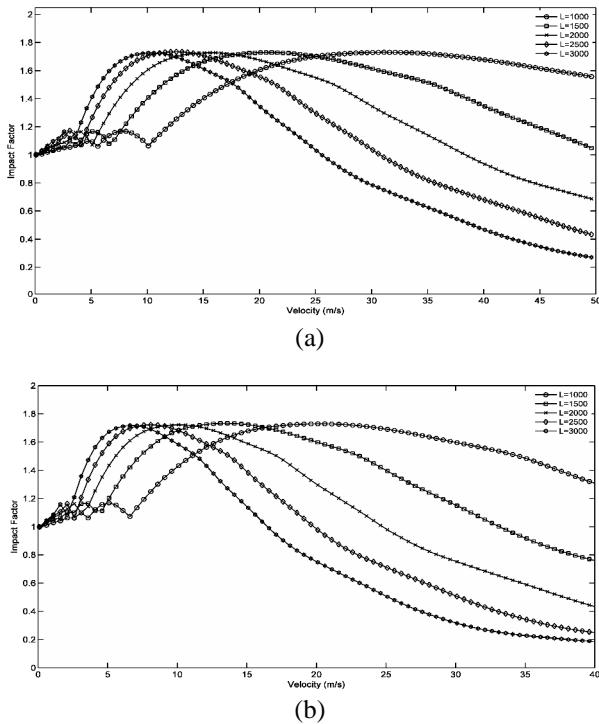


Figure 4. Velocity-impact factor for tunnel with $k=0$, a) ignoring FSI, b) considering FSI in deep water

Accounting for tethers stiffness, modeled as continuous elastic stiffness, the critical speed increases drastically. Figure 5 depicts impact factor evolution as a function of moving load speed in deep and shallow waters ($d_1/d=0.9$) for $k=50$ KN/m/m. Tethers stiffness has great impact on the response, for example in the case of deep water the critical speed increases to about 92 m/s (about 330 Km/h), while for shallow water this speed becomes 72 m/s (about 259 Km/h). This reduction in critical velocity for shallow water indicates that in the case of shallow depth straits, closeness of the tunnel to the sea bed could have significant impact on the dynamic response of the tunnel.

As it is evident from Figure 5, the critical speed becomes nearly constant for tunnels of different length. For the case of deep waters the critical velocity is about 80-100 m/s, while for the case of shallow waters ($d_1/d=0.9$) this reduces to 60-80 m/s.

Comparison of Figures 4 and 5 show the opposite effect of added mass and tether stiffness on the critical speed of the tunnel. While added mass decreases the critical velocity, any increase in tether stiffness increases this velocity. This shows

that how important is the tethers stiffness on the tunnel response and how it can be employed to control the response of the tunnel due to moving loads. Also note that increasing tether stiffness from 0 to 50 KN/m/m, the maximum impact factor corresponding to the critical speed increases from 1.7 to 3, well above the maximum impact factors proposed by codes (e.g. [16]).

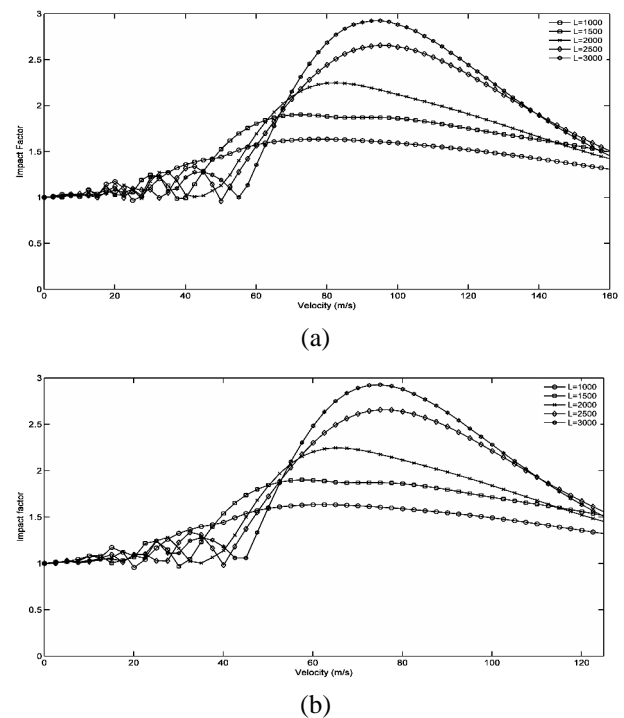


Figure 5. Velocity-impact factor for tunnel with $k=50$ KN/m/m, a) ignoring FSI, b) considering FSI in deep water.

In real applications of the SFTs, the spacing of the tethers could be large, so large that it will be impossible to model its stiffness as a continuous stiffness. For example, as mentioned above, Remseth et al. adopted a tether spacing of 300 m in their study on HØgsfjorden crossing. The boundary condition for each tunnel segment will be something between hinged and fixed conditions. To study the impact of tether spacing at this range in Figure 6 the velocity-impact factor diagram is developed for tunnels of 250 and 500 m long submerged in deep water ($k=0$). As could be seen the critical speed for 250 and 500 m long tunnels in the case of hinged boundary condition will be

about 72 and 36 m/s (252 and 130 Km/h), respectively. These velocities are in the range of the velocity of the vehicles currently in use. At the same time, the impact factor is about 1.7. This shows that in the case of large spacing of the tethers, the effect of moving load on the response becomes outstanding.

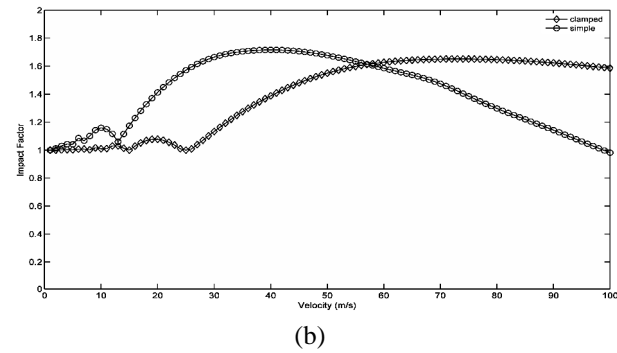
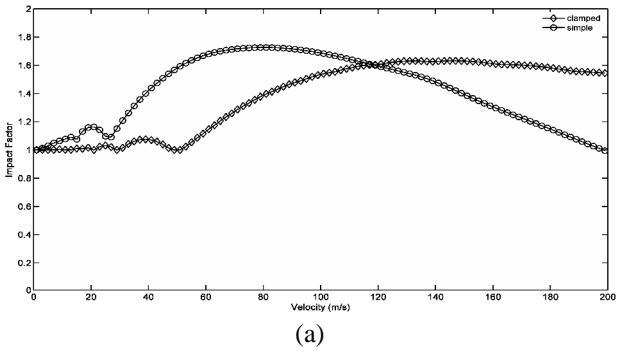


Figure 6. Effect of boundary condition and tether spacing on the velocity-impact factor for tunnels of, a) 250 m long, b) 500 m long.

Figure 7 depicts the change in the frequency of the first seven modes as the tunnel length increases for the case of deep water with $k=50$ KN/m/m. It shows that increasing the tunnel length, the frequency of all modes decreases, while the rate of change for higher modes is higher. This is an indication of larger contribution of higher modes in overall response for longer tunnels. To verify this, we decompose the response in terms of contribution of different modes using analytical response derived in Equation (12). As is evident in this equation, at each mode there is two components, a component with natural frequency and the second one with driving frequency. Closeness of these frequencies for each mode increases the mode contribution in overall response.

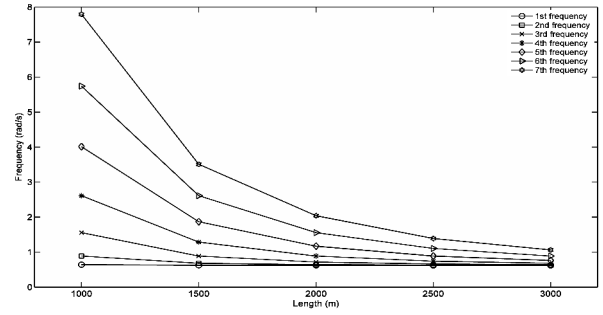


Figure 7. Evolution of first seven modes frequency due to increase in the tunnel length in deep water with $k=50$ KN/m/m.

Figure 8 depicts the modal contribution for tunnel of 1000 and 3000 m in length for moving load velocity of 100 m/s in the case of deep water with $k=50$ KN/m/m. While the main contribution in the case of tunnel of 1000 m in length is from first mode, for tunnel of 3000 m in length the main contribution is from the second mode.

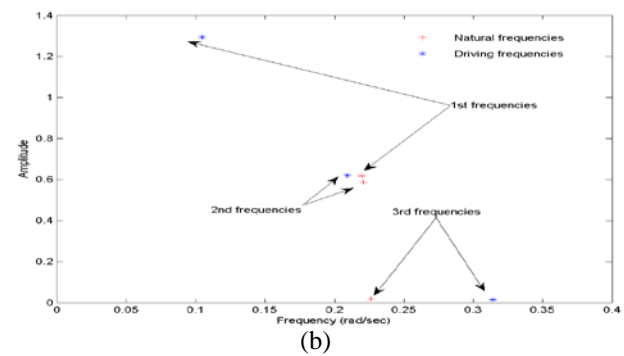
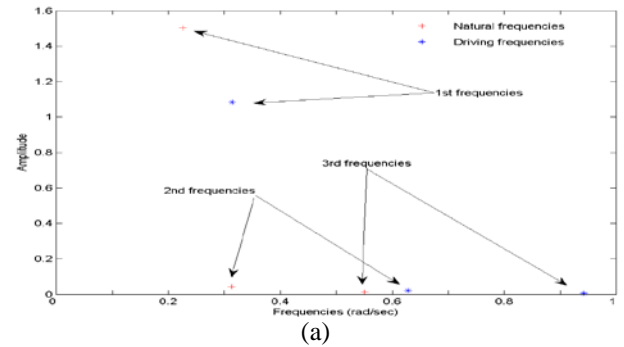


Figure 8. Frequency contribution of different modes in natural and driving frequencies for moving load speed of 100 m/s ($k=50$ KN/m/m), a) tunnel of 1000 m in length, b) tunnel of 3000 m in length.

To have a closer look at the variation of the modes vibration frequencies in Figure 9, the change in the frequency of first mode is depicted for the case of $k=0$ and $k=50$ KN/m/m as function of the tunnel length. The frequency of first mode for the case of $k=50$ KN/m/m remains essentially constant, while for the case of $k=0$ the frequency of the first mode decreases as the tunnel length increases. This indicates that the tether stiffness controls the stiffness of the tunnel. It again demonstrates that for tunnels of large in length, the tether stiffness could be used as a means to control the response of the tunnel due to dynamic loads.

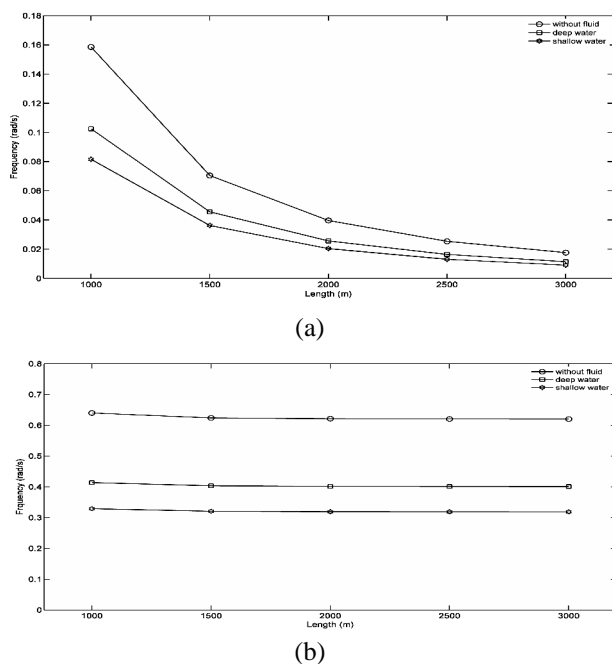


Figure 9. Variation of first mode frequency with tunnel length for different models, a) $k=0$, b) $k=50$ KN/m/m.

4. CONCLUSION

Deriving the added mass for submerged floating tunnel in the case of deep and shallow water, the response of the tunnel to moving load is investigated. Accounting for added mass effect of the surrounding water the critical velocity decreases. It is found that proximity to the sea bed especially in the case of shallow water could substantially decrease the critical velocity. At the same time, while increasing the tether stiffness increases the critical velocity, it also increases the dynamic amplification factor well above the values

commonly envisaged by the Codes.

6. REFERENCES

- Ostlid, H., "Submerged floating tunnel (SFT), a new type of structures for efficient transport", *Energy saving, minimizing pollution and environmental impact*, 4th proceeding of Strait Crossings, (2001).
- FEHRL, "Analysis of the submerged floating tunnel concept", FEHRL report No. 1996/2.a, (1996).
- Remseth, S., Leira, B.J., Okstad, K.M., Mathisen, K.M. and Hawcas, T., "Dynamic response and fluid-structure interaction of submerged floating tunnel", *Journal of Computer and Structure*, Vol. 72, (1999), 659-685.
- Di Pilato, M., Feriani, A. and Perotti, F., "Numerical models for the dynamic response of submerged floating tunnels under seismic loading", *Journal of Earthquake Engineering and Structural Dynamic*, Vol. 37, (2008), 1203-1222.
- Fleischer, D. and Park, S-K., "Plan hydroelastic beam vibration due to uniformly moving one axle vehicle", *Journal of Sound and Vibration*, Vol. 273, (2004), 585-606.
- Paik, B.Y., "Analysis of wave force induced dynamic response of submerged floating tunnel", *KSCCE Journal of Civil Engineering*, Vol. 8, (2004), 543-549.
- Yadykin, Y., Tenetov, V. and Levin, D., "The added mass of a flexible plate oscillating in a fluid", *Journal of Fluids and Structure*, Vol. 17, (2003), 115-123.
- Clark, D., "Calculation of the added mass of circular cylinders in shallow water", *Journal of Ocean Engineering*, Vol. 28, (2001), 1265-1294.
- Clark, D., "Calculation of the added mass of elliptical cylinders with vertical fins in shallow water", *Journal of Ocean Engineering*, Vol. 30, (2002), 1-22.
- Zhou, Z.X., Lo, E.Y.M. and Tan, S.K., "Effect of shallow and narrow water on added mass of cylinder with various cross-sectional shapes", *Journal of Ocean Engineering*, Vol. 32, (2005), 1199-1215.
- Yang, Y.B. and Lin, C.W., "Vehicle-bridge interaction dynamics and potential applications", *Journal of Sound and Vibration*, Vol. 284, (2005), 205-226.
- Pesterev, A.V., Bergman, L.A., Tan, C.A., Tsao, T.C. and Yang, B., "Some recent results in moving load problems with application to highway bridges", (Keynote Lecture delivered by L. A. Bergman), 6th International Conference on Motion and Vibration Control (MOVIC), Saitama, Japan, August (2002).
- Newman, J.N., "Marine Hydrodynamics", 3rd ed. MIT Press, Cambridge, Massachusetts and London, England, (1985).
- Garrison, C.J., "Added mass of a circular cylinder in contact with a rigid boundary", *Hydrodynamics*, Vol. 6. No. 1, (1972), 59-60.
- DNV, "DNV Rules for Submarine Pipeline Systems", Det Norske Veritas, (1981).
- AASHTO, "AASHTO LRFD bridge design specifications", 4th edition, American Association of State Highway and Transportation Officials, (2007).